

SYNTHESIS AND CHARACTERIZATION OF GRAPHENE OXIDE/GOLD NANOPARTICLES/DIBENZOTHIOPHENE HETEROGENEOUS NANOSTRUCTURES

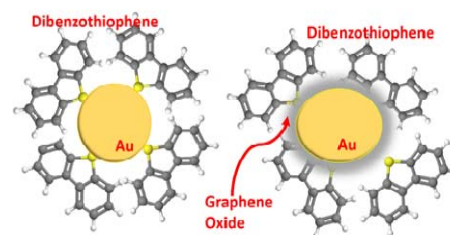
Fatma Bayrakçeken NİŞANCI^{a,b,*}

^a Narman Vocational School, Ataturk University, 25530, Erzurum, Turkey

^b Faculty of Science, Department of Chemistry, Ataturk University, 25240, Erzurum, Turkey

Received January 8, 2020

This work examines the effect of gold nanoparticle (Au NP)- graphene oxide (GO) on the adsorption of dibenzothiophene (DBT) compounds. Au NP-GO were also used as an absorbent to produce nanoscale samples of DBT self-assembled monolayers (SAMs) on Au NP-GO. The influences of DBT adsorption on the size and the time of patterns were investigated. Atomic force microscopy (AFM) and Transmission electron microscopy (TEM) measurements showed that all of the uniformly distributed on Au NP- GO preliminary results indicated that the diameter and the density of DBT adsorptive can be controlled by controlling concentration of GO and Au NP and adsorption time during DBT the stage of SAMs. Photocatalytic oxidation of DBT was studied over Au NPs incorporated DBT Au NP-GO- DBT catalyst under UV radiation.



INTRODUCTION

Dibenzothiophene (DBT, a typical sulfur compound) were chosen as the model compounds and their adsorption over a gold nanoparticle (Au NP) and graphene were committed. The adsorption amounts of DBT over both adsorbents were enhanced which clearly demonstrated that a combination of oxidation and adsorption is better than direct adsorption to achieve a better desulfurization performance. Adsorption of DBT nanostructures with controlled shape and size at predetermined locations on surface has become critically important as the size of devices reaches. Furthermore, model fuels with varied hydrocarbon compositions were employed to investigate the impact of area amounts on the adsorption DBT model compounds and performed their adsorption over two Au NP- graphene oxide (GO).

Sulfur compounds present in liquid hydrocarbon fuels may have a detrimental impact on the environment¹ and human health sulfones can be further removed by adsorption or extraction.¹⁻⁵ Adsorption, which is a well-known process for the removal of pollutants such as heavy-metal ions⁶⁻¹⁰ and hazardous coloring agents¹¹⁻¹⁴ is widely used for reasons including simplicity of operation, ease of design and universal application.¹³ Various conventional adsorbents including diatomite, alumina,¹⁴⁻¹⁶ silica,¹⁷ activated carbon¹⁸ have been tested for the removal of sulfones from oxidized transportation fuels. The adsorption amounts over them were found to be at least 2 times higher than those of commercial silica gel and activated carbon.¹⁹ Hybrid materials based on inorganic nanoparticles and graphene on its hydrophilic derivative, (GO) have been shown as a promising research area, utilizing a combination of properties

* Corresponding author: fbayrakceken@atauni.edu.tr

such as high specific surface area, light weight, chemical inertness mechanical robustness and excellent electrical and thermal conductivity.²⁰⁻²² The functionality of the resulting Au NP-GO hybrids is assessed for the commercially important adsorption of DBT example of applying inorganic Au NP-GO hybrids to adsorption.^{23,24}

EXPERIMENTAL

Au (99.99 %) used as a target and argon gases were used as the sputtering gases. The base pressure was $< 3.0 \times 10^{-4}$ Pa. During deposition, the substrate (glass) at room temperature was maintained with a sputtering power of 20 V. Au thin films on the glass with thickness ranging from 80 to 200 nm were obtained after a deposition time to 25 sec-1000 sec. The experimental conditions were as follows; sputtering time 25 sec-1000 sec; applied voltage 20 V, respectively. GO (aqueous dispersion, 4.0 mg/mL) was purchased from Sigma Aldrich. The GO layer was formed by dropping Au-glass thin film from 2.0 mg/mL GO aqueous dispersion. 1- Dibenzothiophene (DBT) were prepared by immersion of Au thin film-GO sheet in solutions containing 10.0 mM DBT (Fluka, purity $\geq 97\%$) for 24 h. Surface morphological studies of composites were examined and measured by scanning electron microscopy (SEM, Zeiss Sigma 300). Ultraviolet-visible (UV-Vis) spectroscopy measurements were obtained from a Shimadzu UV-3600 Plus spectrophotometer. The surface characterization of the films prepared by TEM (Transmission Electron Microscopy) and AFM (Atomic Force Microscopy) images was made possible to investigate the surfaces in atomic and molecular dimensions and Hitachi HT770 brand TEM and Hitachi S100N brand AFM systems were used respectively. For the purpose of the surface analysis, the particles were coated on gold using a sputter coater (Q150V Plus, Series from Quorum Technologies). The photocatalytic oxidation reaction was conducted in the batch photo-reactor that was purchased from (model VG-500) Sen Light Corporation. The radiation source used was 100 W emitting maximum intensity at 365 nm. The lamp was fitted inside the reactor. The reactor set up was covered with aluminum foil to prevent UV light leakage. The reactor is provided with an inlet and outlet for aeration and water cooling system.

The reactant solution used in each experiment was prepared by adding isooctane solution to give an elemental sulfur concentration (dibenzothiophene) at a desire level. In a typical experiment, different thickness samples of Au-GO-DBT films in isooctane solution were added to the reactor and

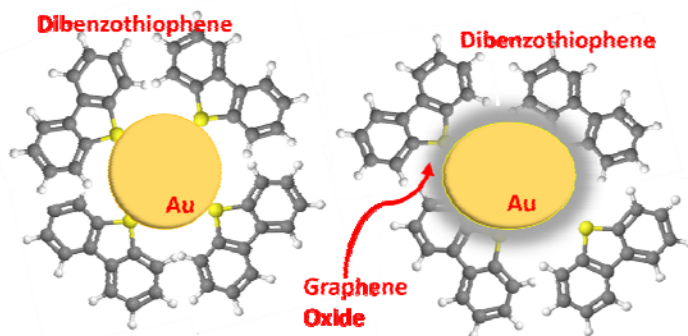
kept for about 30 min with stirring to achieve the equilibrium. After this time, hydrogen peroxide (30.0 wt% H_2O_2) was added to the mixture and the reaction started (zero time). Small amount of samples were collected periodically from the isooctane phase for monitoring the progress of reaction for quantitative analysis of thiophenic sulfur compound in organic phase. After the oxidation of dibenzothiophene, this confirms that the oxidized products were transferred to the water phase from the organic phase. This dibenzothiophene was used in the reaction and the progress of the reaction was monitored by measuring the reduction of concentration of sulfur compounds in the isooctane layer.

RESULTS AND DISCUSSION

The adsorption behaviors of DBT over the two adsorbents were found to be significantly different. Besides, it was found that Au NP performed better for DBT removal compared to GO but the adsorption amount of DBT over Au NP-GO exceeded the corresponding value over Au NP. Show that the adsorption kinetics of DBT SAMs follows the 2D instantaneous nucleation and grow in surface. Figure 1 shows that in the TEM image of Au-GO-DBT nanostructures, DBT structures are disc shaped and distributed evenly on surfaces.

These images recorded for different deposition times indicate that the thickness of DBT increase until a certain thickness and diameter of DBT adsorptive increases and covers the surface completely at longer times.

Before adsorption of DBT, we intended to obtain AFM images of the aggregate formed by the procedure described above our attempts to obtain clear images of adsorption centers on GO-Au modified surfaces consistently successful while we managed to get high resolution AFM images of DBT modified GO- Au surface (Figure 2). Figure 2 a shows adsorption behavior of DBT covered GO-Au electrode in solution containing 10.0 mM DBT after application in the potential step with a pulse width of 200 s and potential 80 V and GO modified on the glass.



Scheme 1 – Schematic illustration of the experimental strategy to fabricate the patterned GO-Au nanostructures-DBT SAMs.

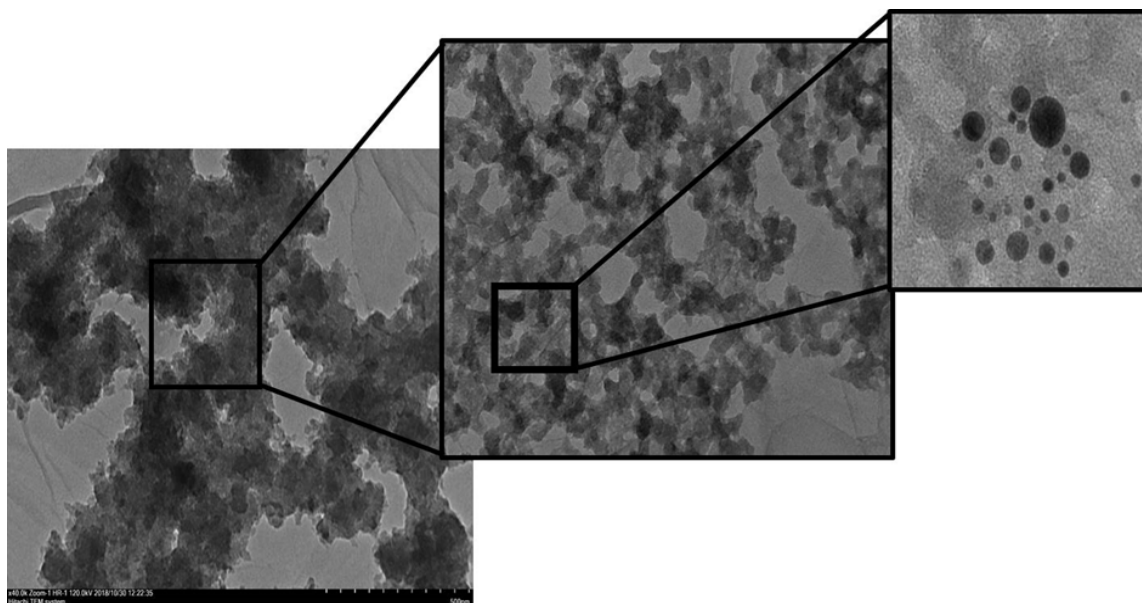


Fig. 1 – TEM micrographs of GO-Au NPs-DBT thin film.

The morphological study of the prepared adsorbents was carried out with atomic force microscopy (AFM) in order to check its surface and porosity. Pores present in the adsorbent surface have high role in the adsorbate adsorption. Generally, the adsorbent with porous and rough morphology has high adsorption capacity. Figure 2 shows the AFM images of 2.0 mg GO-80 V 200 s Au-DBT (10.0 mM), 80 V 200 s Au-DBT (10.0 mM) and 2.0 mg GO thin films formed on glass substrates. From the figures it can be seen that Au nanoparticle film thickness rise has increased the porosity of the DBT which has a positive effect on its adsorption capacity. Because pores present on the adsorbent surface reduce resistance to adsorbed molecules and also facilitate their diffusion from solutions to adsorbent surface. The surface of DBT loaded with magnetite nanoparticles is also porous but along with porous structure, its surfaces also seems very rough, due to rough and porous structure, its adsorption capacity will be more than 2.0 mg GO thin film. Thus, the AFM images of 2.0 mg GO-80 V 200 s Au-DBT (10.0 mM), 80 V 200 s Au-DBT (10.0 mM) and 2.0 mg GO thin films strongly supported by the experimental results.

Figure 3 shows that the number of DBT adsorption increases amplitude of the potential step of Au NPs. This increment in the number of DBT adsorbents with the increase in potential step amplitude results in the formation of more Au NPs on GO monolayers due to the increase in the rate of Au NP centers formation. The AFM images of DBT adsorbent obtained after modified of Au NP at different potential step pulse widths are shown in Figure 3 a-d. The potential step pulse widths are

25 s, 50 s, 100 s, 500 s and constant potential 20 V. Sequential images show that the number of disk-shaped DBT adsorbents increases with the increase in potential pulse width, while DBT adsorbent diameters remain almost constant. Figure 3 d shows that DBT adsorbents cover the surface almost completely after 500 s of coating of Au. In AFM hybrid materials, GO (Figure 3) suggests the presence of well-exfoliated GO layers covered by fully functional nanoparticles.

Figure 4 shows the UV-vis absorption spectra of GO- AuNPs decorated with DBT. The peak at the 527.5 nm can be attributed to the presence of AuNPs. The peaks at about 230 and 300 nm belong to GO, the first peak is related to π to π^* transition of the aromatic carbons and the second peak arises from the n to π^* transition of the carbonyl group. Further confirmation of the attachment of DBT on the GO-Au NPs was achieved by spectroscopic study of the addition of free AuNPs to the suspension of AuNPs-DBT-GO. Based on the illustrated absorption spectra of AuNPs-DBT-GO, there is no free AuNPs, therefore, almost all of the AuNPs were attached to the DBT-GO. In addition, comparison between the low and high concentrations of AuNPs (in AuNPs-DBT-GO) indicates that a more clear shoulder peak appears at about 300 nm at the higher concentration of the nanoparticles. A small red shift of absorbance spectra was observed after Au coating. This indicates a decrease in band gap energy of GO/Au (2.0 mg GO- 500 s Au- DBT (10.0 Mm) thin films) catalyst. But the decrease in band gap energy is much smaller than the previous reports.^{21–23}

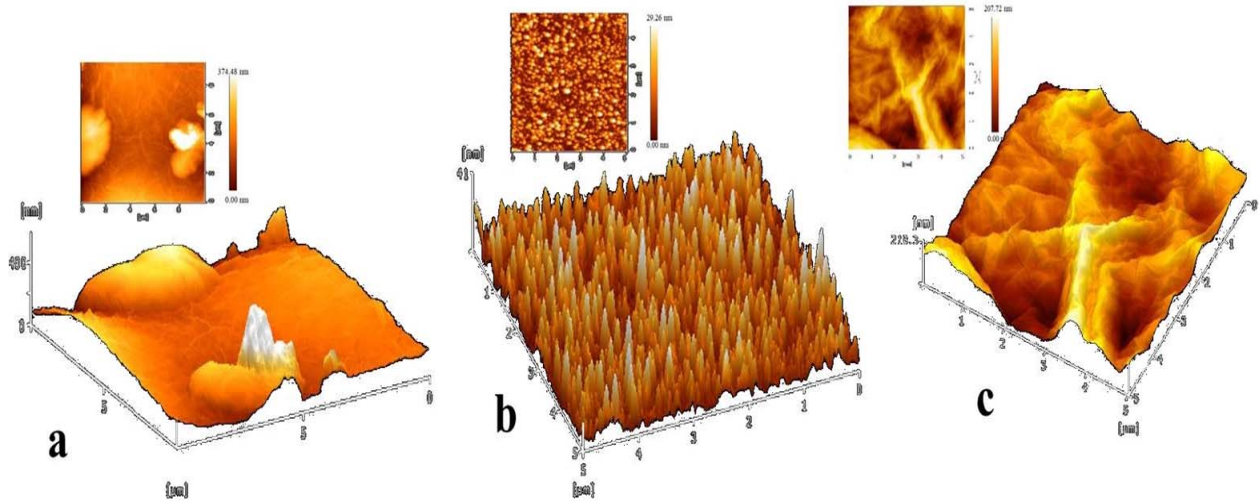


Fig. 2 – (a-c) AFM images of a) 2.0 mg GO-80 V 200 s Au-DBT (10.0 mM), (b) 80 V 200 s Au-DBT (10.0 mM) and (c) 2.0 mg GO thin films formed on glass substrates.

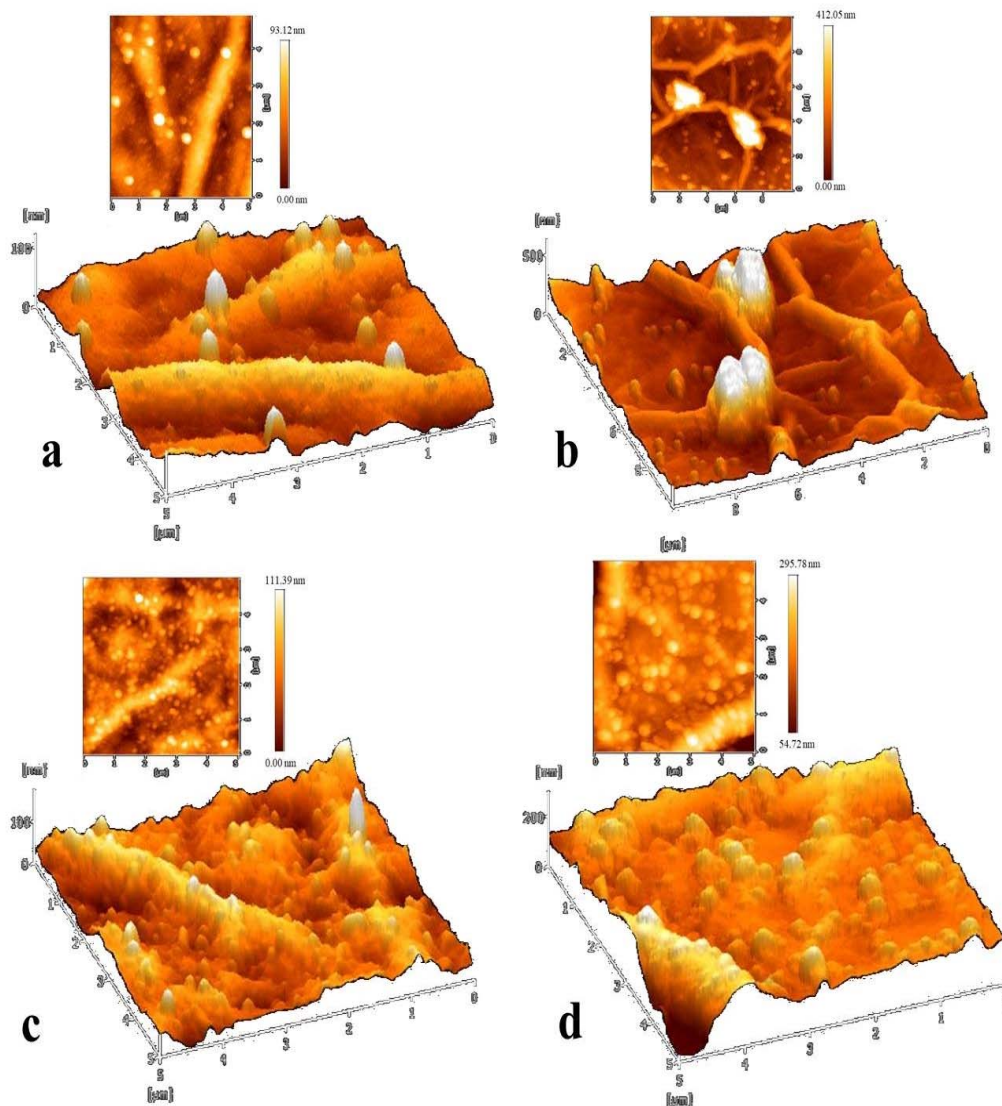


Fig. 3 – (a-d) AFM images of a) 2.0 mg GO-20 V 25 s Au-DBT (10.0 mM), (b) 2.0 mg GO-20 V 50 s Au-DBT (10.0 mM), (c) 2.0 mg GO-20 V 100 s Au-DBT (10.0 mM) and (d) 2.0 mg GO-20 V 500 s Au-DBT (10.0 mM) thin films formed on glass substrates.

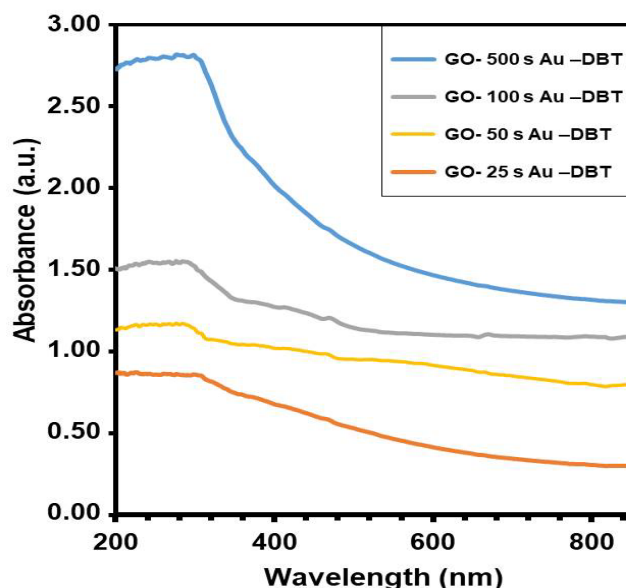


Fig. 4 – UV-Visible absorption spectra of 2.0 mg GO- 25 s Au- DBT (10.0 mM), 2.0 mg GO- 50 s Au- DBT (10.0 mM), 2.0 mg GO- 100 s Au-DBT (10.0 mM) and 2.0 mg GO- 500 s Au- DBT (10.0 mM) thin films formed on glass substrates.

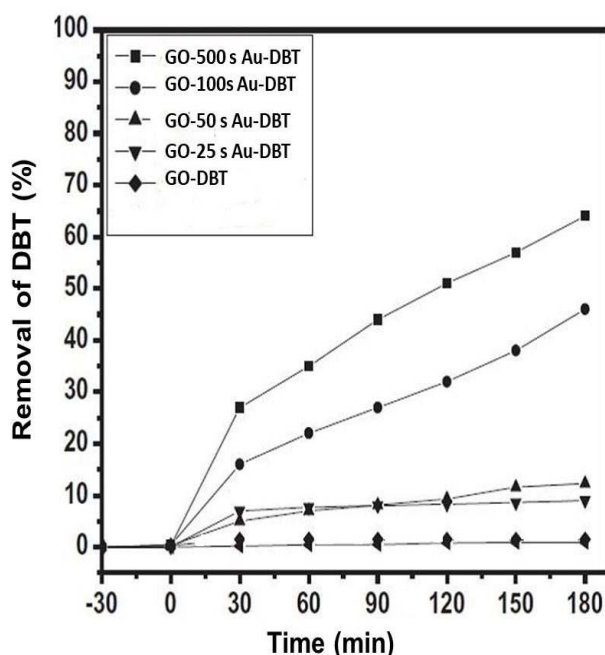


Fig. 5 – The photocatalytic removal of DBT in 2.0 mg GO- 25 s Au- DBT, 2.0 mg GO- 50 s Au- DBT, 2.0 mg GO- 100 s Au-DBT and 2.0 mg GO- 500 s Au- DBT catalysts.

The efficiency of removal of DBT under different surface conditions are presented in Figure 5. The removal of DBT is negligible under UV direct photolysis and under dark condition with GO-DBT and GO-Au different thicknesses –DBT. The removal of DBT under direct photolysis is 0.9%. 2.0 mg GO- 500 s Au- DBT (10.0 mM) systems showed higher efficiency to remove the DBT. Decomposition of H_2O_2 under UV irradiation leads to OH^\cdot formation, which takes

part in oxidation of DBT. When H_2O_2 was employed with the photocatalytic system of GO-100 s Au-DBT/UV, a significant increase % removal of DBT (43%) was observed.

In addition, the efficiency of the removal of DBT was improved by doping Au on GO. When the noble metal Au is introduced into pure GO, Au acts as electron traps and minimizes the electron-hole recombination. The electron transfer from the GO conduction band to metallic gold particles at

the interface is possible and thus prevents the electron-hole recombination, which enhances the photocatalytic activity of the GO/Au catalyst. In addition, the Au NPs help the decomposition of H_2O_2 , thereby increase the hydroxyl radicals, which in turn increase the removal of DBT. It is important to note that comparison of photocatalytic removal of DBT showed that the sulfur removal could reach 59% for DBT after 180 min.

CONCLUSIONS

Au NP and GO have been applied for the adsorption of DBT from model fuels with different hydrocarbon compositions. The nonreactive adsorption performance of AuNP-GO materials for sulfur removal from aqueous hydrocarbons was studied by investigating DBT adsorption onto AuNP-GO adsorbents. Synthesis of Au NP-GO adsorbents was achieved through precipitation of GO sheets onto exfoliated Au NP followed by spatter and immersion. Au NP-GO likely act as effective spacer between the adsorbent particles, leading to improved accessibility of active adsorption sites, resulting in significantly enhanced organosulfur uptake. Additionally the cycle, stability of the pure Au NP-GO was enhanced by the addition of GO due to robust binding between the change complementary hybrid components, inhibiting Au NP-GO particle sintering during adsorbent regeneration. The adsorption behaviors of DBT over the two adsorbents were found to be significantly different. The images recorded for different deposition times indicate that the thickness of DBT increase until a certain time, and diameter of DBT adsorptive increases and covers the surface completely at longer times. The result demonstrated that the great improvement on the increase of the surface attachment response at 2.0 mg GO-20 V 500 s Au- DBT was attributed to the satisfactory synergic effect of 2.0 mg GO-20 V 500 s Au NPs, which was due to the excellent characteristics of the NPs such as high electrical conductivity, high surface area and more electroactive interaction sites for electron transfer and charge exchange between the analyte and the modified electrode surface.

REFERENCES

1. Y. Shi, G. Liu and X. W. Zhang, *Ind. Eng. Chem. Res.*, **2017**, 56, 2557-2164.
2. Y. Zhu, M. Zhu, L. Kang, F. Yu and B. Dai, *Ind. Eng. Chem. Res.*, **2015**, 54, 2040–2047.
3. Y. Shi, G. Liu, B. Zhang and X. Zhang, *Green Chem.*, **2016**, 18, 5273–5279.
4. W. Liu, W. Jiang, W. Zhu, W. Zhu, H. Li, T. Guo, W. Zhu and H. Li, *J. Mol. Catal. A: Chem.*, **2016**, 424, 261–268.
5. M. C. Lu, L. C. C. Biel, M. W. Wan, R. de Leon, S. Arco and C. M. Futralan, *Desalin. Water Treat.*, **2016**, 57, 5108–5118.
6. V. Gupta, S. Srivastava, D. Mohan and S. Sharma, *Waste Manage.*, **1998**, 17, 517–522.
7. V. K. Gupta, A. Nayak and S. Agarwal, *Environ. Eng. Res.*, **2015**, 20, 1–18.
8. V. K. Gupta, S. Agarwal and T. A. Saleh, *J. Hazard. Mater.*, **2011**, 185, 17–23.
9. V. K. Gupta and A. Nayak, *Chem. Eng. J.*, **2012**, 180, 81–90.
10. T. A. Saleh and V. K. Gupta, *Environ. Sci. Pollut. Res.*, **2012**, 19, 1224–1228.
11. A. K. Jain, V. K. Gupta, A. Bhatnagar and A. Suhas, *Sep. Sci. Technol.*, **2003**, 38, 463–481.
12. A. Mittal, J. Mittal, A. Malviya and V. K. Gupta, *J. Colloid Interface Sci.*, **2009**, 340, 16–26.
13. A. Mittal, J. Mittal, A. Malviya and V. K. Gupta, *J. Colloid Interface Sci.*, **2010**, 344, 497–507.
14. A. Mittal, J. Mittal, A. Malviya, D. Kaur and V. K. Gupta, *J. Colloid Interface Sci.*, **2010**, 342, 518–527.
15. A. Ishihara, D. Wang, F. Dumeignil, H. Amano, E. W. Qian and T. Kabe, *Appl. Catal.*, **2005**, 279, 279–287.
16. O. Etemadi and T. F. Yen, *Energy Fuels*, **2007**, 21, 1622–1627.
17. M. C. Lu, M. L. Agripa, M. W. Wan and M. L. P. Dalida, *Desalin. Water Treat.*, **2014**, 52, 873–879.
18. S. Sato, K. Yazu and A. Matsumura, *J. Jpn. Pet. Inst.*, **2006**, 49, 210–213.
19. S. M. Lim, J. N. Kim, J. Park, S. S. Han, J. H. Park, T. S. Jung, H. C. Yoon, S. H. Kim and C. H. Ko, *Energy Fuels*, **2012**, 26, 2168–2174.
20. A. Nanoti, S. Dasgupta, A. N. Goswami, B. R. Nautiyal, T. V. Rao, B. Sain, Y. K. Sharma, S. Nanoti, M. O. Garg and P. Gupta, *Microporous Mesoporous Mater.*, **2009**, 124, 94–99.
21. R. Memci, D. Iruretagoyera, V. Wang, S. M. Poawolad, M. Mozehter, S. A. Al thabasto, S. N. Bshal, M. S. Shafter and A. K. Geim, *Science*, **2009**, 324, 1530-1534.
22. F. W. Chang, Y. Hsin-Yin, L. S. Roselin, H. C. Yang and T. C. Ou, *Appl. Catal. A*, **2006**, 302, 157-167.
23. V. P. Kamat, *Pure Appl. Chem.*, **2002**, 74, 1693-1706.
24. V. Subramanian, E. E. Wolf and V. P. Kamat, *J. Am. Chem. Soc.*, **2004**, 126, 4943-4950.